

# **Geophysical Research Letters**\*

# ᢙ

# **RESEARCH LETTER**

10.1029/2021GL097125

#### **Key Points:**

- Near real-time photogrammetric monitoring of the 2021 Fagradalsfjall eruntion
- Acquisition of an unprecedented temporal data set including volume, effusion rate, orthomosaics, thickness maps and thickness change maps
- By the end of the eruption the lava covered 4.8 km<sup>2</sup>, with a bulk volume of ~1.5 × 10<sup>8</sup> m<sup>3</sup> and mean output rate of ~9.5 m<sup>3</sup>/s

#### **Supporting Information:**

Supporting Information may be found in the online version of this article.

#### Correspondence to:

G. B. M. Pedersen, gro@hi.is

#### Citation:

Pedersen, G. B. M., Belart, J. M. C., Óskarsson, B. V., Gudmundsson, M. T., Gies, N., Högnadóttir, T., et al. (2022). Volume, effusion rate, and lava transport during the 2021 Fagradalsfjall eruption: Results from near real-time photogrammetric monitoring. *Geophysical Research Letters*, 49, e2021GL097125. https://doi. org/10.1029/2021GL097125

Received 1 DEC 2021 Accepted 3 JUN 2022

#### **Author Contributions:**

Joaquin M. C. Belart, Birgir Vilhelm Óskarsson, Magnús Tumi Gudmundsson **Data curation:** Joaquin M. C. Belart, Birgir Vilhelm Óskarsson, Nils Gies, Thórdís Högnadóttir **Formal analysis:** Gro B. M. Pedersen, Joaquin M. C. Belart, Birgir Vilhelm Óskarsson, Magnús Tumi Gudmundsson, Nils Gies, Thórdís Högnadóttir, Virginie Pinel. Etienne Berthier

Conceptualization: Gro B. M. Pedersen,

© 2022. The Authors.

This is an open access article under the terms of the Creative Commons Attribution License, which permits use, distribution and reproduction in any medium, provided the original work is properly cited.

# Volume, Effusion Rate, and Lava Transport During the 2021 Fagradalsfjall Eruption: Results From Near Real-Time Photogrammetric Monitoring

Gro B. M. Pedersen<sup>1</sup>, Joaquin M. C. Belart<sup>2,3</sup>, Birgir Vilhelm Óskarsson<sup>4</sup>, Magnús Tumi Gudmundsson<sup>1</sup>, Nils Gies<sup>4,5</sup>, Thórdís Högnadóttir<sup>1</sup>, Asta Rut Hjartardóttir<sup>1</sup>, Virginie Pinel<sup>6</sup>, Etienne Berthier<sup>7</sup>, Tobias Dürig<sup>1</sup>, Hannah Iona Reynolds<sup>1</sup>, Christopher W. Hamilton<sup>1,8</sup>, Guðmundur Valsson<sup>2</sup>, Páll Einarsson<sup>1</sup>, Daniel Ben-Yehosua<sup>9</sup>, Andri Gunnarsson<sup>10</sup>, and Björn Oddsson<sup>11</sup>

<sup>1</sup>Nordic Volcanological Center, Institute of Earth Sciences, University of Iceland, Reykjavík, Iceland, <sup>2</sup>National Land Survey of Iceland, Akranes, Iceland, <sup>3</sup>Institute of Earth Sciences, University of Iceland, Reykjavík, Iceland, <sup>4</sup>Icelandic Institute of Natural History, Garðabær, Iceland, <sup>5</sup>Institute of Geological Sciences, University of Bern, Bern, Switzerland, <sup>6</sup>CNRS, IRD, Université Gustave Eiffel, Université Grenoble Alpes, University of Savoy Mont Blanc, Grenoble, France, <sup>7</sup>LEGOS CNRS, University of Toulouse, Toulouse, France, <sup>8</sup>The University of Arizona, University Boulevard Tucson, Tucson, AZ, USA, <sup>9</sup>Faculty of Civil and Environmental Engineering, University of Iceland, Reykjavík, Iceland, <sup>10</sup>The National Power Company of Iceland (Landsvirkjun), Reykjavík, Iceland, <sup>11</sup>The Department of Civil Protection and Emergency Management, Reykjavík, Iceland

**Abstract** The basaltic effusive eruption at Mt. Fagradalsfjall lasted from 19 March to 18 September 2021, ending a 781-year repose period on Reykjanes Peninsula, Iceland. By late September 2021, 33 near real-time photogrammetric surveys were completed using satellite and airborne images, usually processed within 3–6 hr. The results provide unprecedented temporal data sets of lava volume, thickness, and effusion rate. This enabled rapid assessment of eruption evolution and hazards to populated areas, important infrastructure, and tourist centers. The lava flow field has a mean lava thickness exceeding 30 m, covers 4.8 km² and has a bulk volume of  $150 \pm 3 \times 10^6$  m³. The March–September mean bulk effusion rate is  $9.5 \pm 0.2$  m³/s, ranging between 1 and 8 m³/s in March–April and increasing to 9–13 m³/s in May–September. This is uncommon for recent Icelandic eruptions, where the highest discharge usually occurs in the opening phase.

**Plain Language Summary** On 19 March 2021, an eruption began at Mt. Fagradalsfjall after 781 years of dormancy on the Reykjanes Peninsula, Iceland. To monitor and evaluate hazards of the eruption, satellite and airborne stereoimages were processed and made publicly available on the same day as they were surveyed. The data were used to create 3D models of the lava and update the lava volume and growth rate. The resulting maps were used by disaster response teams to evaluate the risk of the lava flow to nearby infrastructure and to manage tourism in the vicinity of the eruption. On 18 September 2021, the new lava flow field covered 4.8 km², was up to 124 m thick and had a mean thickness of 30 m, yielding a total bulk volume of 150 million m³. The mean discharge during the six months of the eruption was 9.5 m³/s, equivalent to filling one Olympic swimming pool every 4 min.

# 1. Introduction

On 19 March 2021, a 6-month subaerial, effusive, basaltic eruption started at Mt. Fagradalsfjall ending a 781-year dormancy on the Reykjanes Peninsula, Iceland (Figure 1). Initially, the eruption started in the valley Geldingardalir, with the lava infilling that valley. Following a phase of active vent migration, the lava flow field expanded into neighboring valleys in the Fagradalsfjall area, which is a complex of intergrown tuyas and tindars formed during subglacial eruptions (e.g., Jones, 1969; Pedersen & Grosse, 2014).

Reykjanes Peninsula is an onshore continuation of the Mid-Atlantic plate boundary and is, together with the Grímsey rift, atypical compared to other Icelandic volcanic zones by being a highly oblique spreading zone. It has N-S trending strike slip faults and volcanic systems consisting of 10–40 km long NE-SW-trending fissure swarms and geothermal areas. Fagradalsfjall volcanic system is an exception displaying none of these characteristics and is the least active volcanic system of the Peninsula (e.g., Clifton & Kattenhorn, 2006; Einarsson

PEDERSEN ET AL. 1 of 11



Funding acquisition: Magnús Tumi Gudmundsson, Virginie Pinel, Etienne Berthier

Investigation: Gro B. M. Pedersen, Joaquin M. C. Belart, Birgir Vilhelm Óskarsson, Magnús Tumi Gudmundsson, Nils Gies, Ásta Rut Hjartardóttir, Virginie Pinel, Etienne Berthier

**Methodology:** Joaquin M. C. Belart, Birgir Vilhelm Óskarsson, Magnús Tumi Gudmundsson, Nils Gies

Project Administration: Gro B. M. Pedersen, Birgir Vilhelm Óskarsson, Magnús Tumi Gudmundsson Resources: Virginie Pinel, Etienne Berthier

**Software:** Gro B. M. Pedersen, Joaquin M. C. Belart

Supervision: Gro B. M. Pedersen Validation: Joaquin M. C. Belart, Magnús Tumi Gudmundsson, Nils Gies Visualization: Gro B. M. Pedersen, Magnús Tumi Gudmundsson, Thórdís Högnadóttir, Ásta Rut Hjartardóttir Writing – original draft: Gro B. M. Pedersen

Writing – review & editing: Gro B. M. Pedersen, Joaquin M. C. Belart, Birgir Vilhelm Óskarsson, Magnús Tumi Gudmundsson, Nils Gies, Thórdís Högnadóttir, Ásta Rut Hjartardóttir, Virginie Pinel, Etienne Berthier et al., 2020, 2022; Gee, 1998; Klein et al., 1977; Sæmundsson et al., 2020). Eruptions on the Peninsula occur from fissures, that may focus into a single vent to form lava shields; volcanic activity over the last 4,000 years has been episodic, with multiple eruptions occurring over several hundred years followed by ~800–1,000 years of quiescence. The previous eruptive period ended in 1240 CE (Sæmundsson et al., 2020).

Lava flows from eruptions on the Reykjanes Peninsula may reach inhabited areas or inundate essential infrastructure. The Fagradalsfjall eruption therefore became a case-study for the monitoring and hazard assessment of future eruptions in the area.

Effusion rates and volumes of lava flows are key eruption parameters necessary for evaluation of hazards posed by effusive basaltic eruptions. They are the main controlling factors for lava emplacement, transport system, advance rate and final lava extent (e.g., Calvari, 2019; Harris et al., 2007; Walker, 1973). They also provide important insight into the dynamics of the magma plumbing systems, including how eruption rates may be controlled by the complex interaction between the magma reservoir and the conduit feeding the eruption (Aravena et al., 2020; Harris et al., 2000, 2011). Various methods exist to monitor and quantify near real-time effusion rate ranging from localized channel and tube estimates of instantaneous effusion rate to time-averaged discharge rate (TADR) using satellite-based thermal data, synthetic aperture radar data and photogrammetric methods (e.g., Dietterich et al., 2021; Harris et al., 2007; Poland, 2014 and references therein).

Here we present a significant achievement in full-scale near real-time photogrammetric monitoring, yielding daily to weekly 3D models of the Fagradalsfjall 2021 eruption, which provided key information necessary for evaluating hazards. This included volume and TADR evolution, and monitoring of the lava extent and valley overflows. Post-eruption, this information has also been used to interpret magma plumbing dynamics.

#### 2. Data and Methods

The data used for near real-time monitoring of the Fagradalsfjall 2021 eruption consists mainly of aerial photographs and Pléiades stereoimages. By 30 September 2021, 33 surveys had been carried out (Table S1 in Supporting Information S1). The airborne photogrammetric surveys of the eruption started on the morning of 20 March 2021, 11 hr after the eruption began. The bulk of surveys were done with a TF-BMW Partenavia P 68 Observer II survey aircraft operated by Garðaflug Corp (Table S1 in Supporting Information S1) with a Hasselblad A6D 100 MP medium-format camera with a 35 mm focal lens. Images were taken vertically at an altitude of 550–1,800 m. a.s.l. with 75%–90% overlap and image resolution of 7–30 cm. Up to 24 ground control points were placed around the lava flow field and measured with a high-precision GNSS instrument (see Text S1–S3 and Figures S1–S3 in Supporting Information S1).

The aerial photographs were processed in the software MicMac (Pierrot Deseilligny & Clery, 2011; Rupnik et al., 2017), following the semi-automated workflow of Belart et al. (2019), as well as in Agisoft Metashape (version 1.7.3) and Pix4D mapper (version 4.6.4). The Pléiades data was processed using the Ames StereoPipeline (Shean et al., 2016). These pipelines yielded the DEMs and orthomosaics for each survey. Each DEM was compared with a pre-eruption DEM ( $2 \times 2$  m) and with the previous survey done, obtaining a thickness map and a thickness change map (Figure S4 in Supporting Information S1).

Lava outlines were manually digitized from the orthomosaics. Volumes were calculated using the mean thickness of the erupted deposit multiplied by its area. The uncertainties of the volume were obtained using the Normalized Mean Absolute Deviation (Höhle & Höhle, 2009) of the stable areas surrounding the lavas, as proxy for the uncertainties of the thickness maps. The uncertainties of the TADR are described in Text S2 of Supporting Information S1.

#### 3. Results

After each survey the data products: DEMs  $(2 \times 2 \text{ m})$ , orthomosaics  $(0.3 \times 0.3 \text{ m})$ , thickness maps  $(2 \times 2 \text{ m})$ , and lava outlines were completed and made available, usually 3–6 hr after acquisition (Figure S4 in Supporting Information S1). Thanks to the short latency of data delivery, the data products became important for the civil protection authorities. Table S2 in Supporting Information S1 provides the results from each survey.

PEDERSEN ET AL. 2 of 11

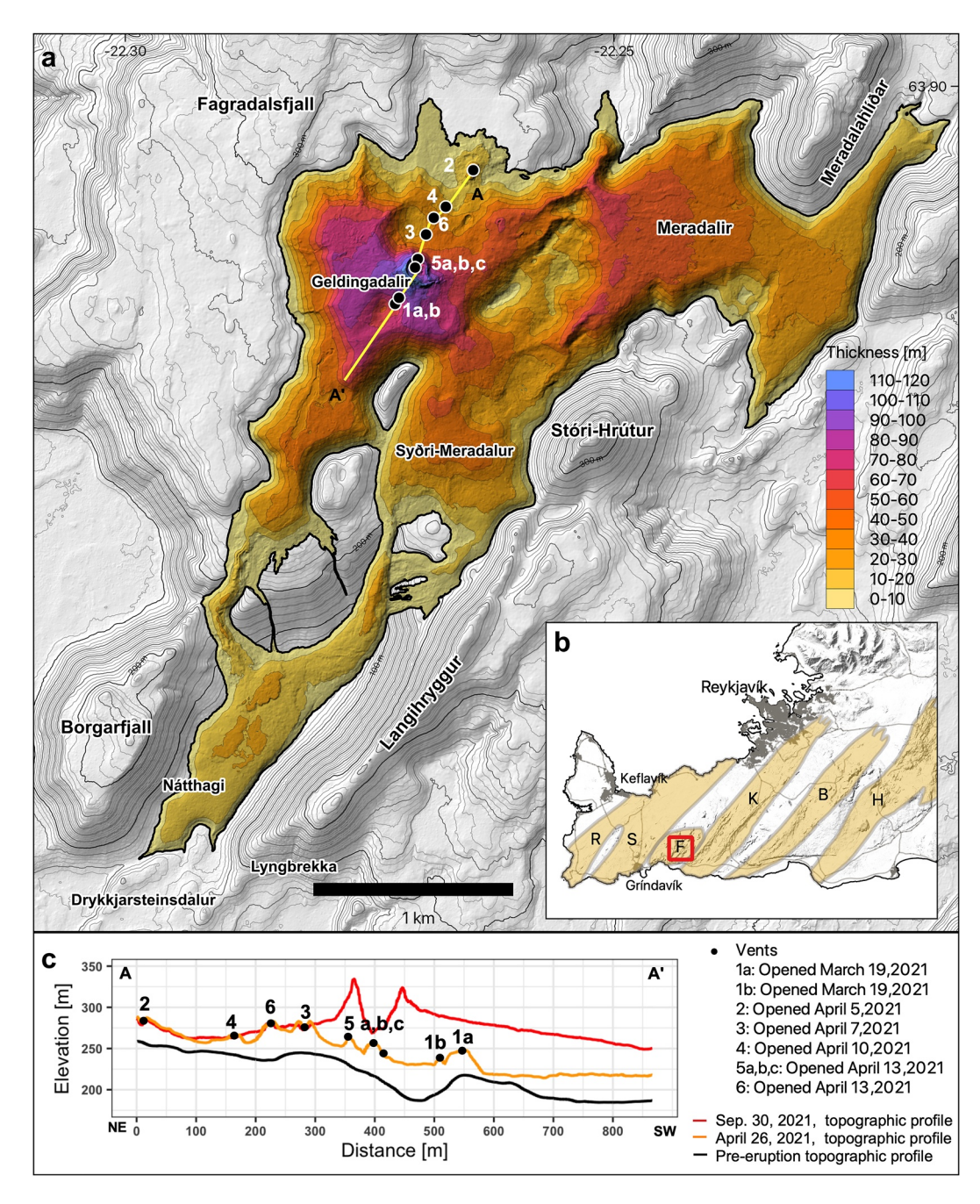


**Figure 1.** (a) Thickness map of the erupted products in the Fagradalsfjall eruption by 30 September 2021. Vents are marked with dots and numbered chronologically after opening time. Location of topographic profile (A-A') in (c) is marked as a yellow line. Background topography is based on IslandsDEM v0. (b) Map of the Reykjanes Peninsula. The red box indicates the area displayed in (a). Densely populated areas are marked in gray. Volcanic systems (Sæmundsson & Sigurgeirsson, 2013) are marked with orange and denoted by capital letter according to their name; R, Reykjanes; S, Svartsengi; F, Fagradalsfjall; K, Krýsuvík; B, Brennisteinsfjöll; H, Hengill. (c) Topographic profile along the vents from NE to SW (location in [a]).

Here, we describe the evolution of the eruption, the erupted volume and bulk TADR, as well as the lava flow field development. Short-term fluctuations (minutes to hours) are not resolved by these measurements.

# 3.1. Fagradalsfjall Eruption: Volume, Discharge and Lava Field Evolution

The eruption from 19 March 2021 to 18 September 2021 can be divided into five phases.

PEDERSEN ET AL. 3 of 11

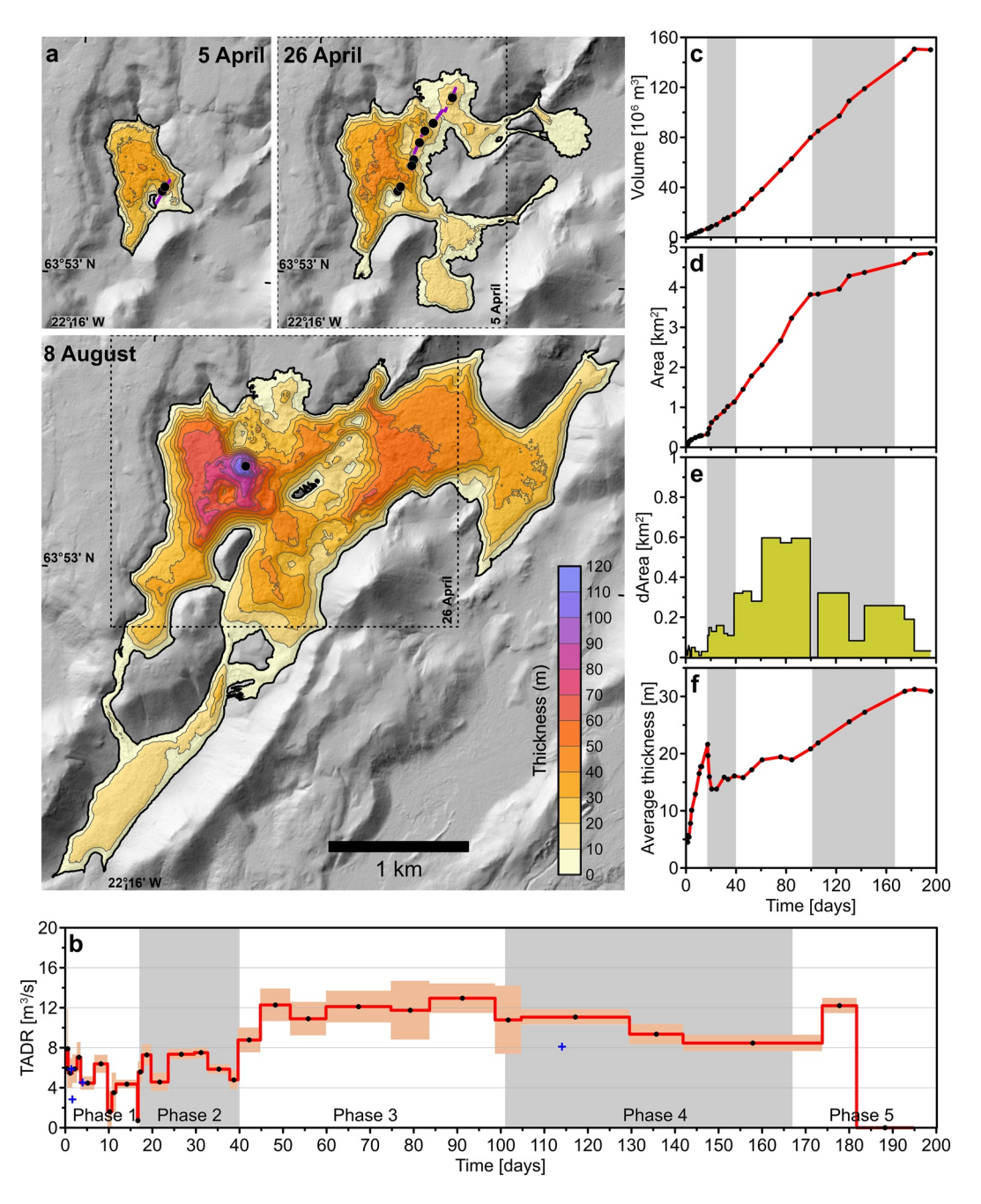


**Figure 2.** (a) The thickness of erupted material by the end of Phase 1 (5 April), end of Phase 2 (26 April) and Phase 4 (8 August 2021). Purple line denotes initial fissure segment. (b–f) Eruption parameters of the Fagradalsfjall 2021 eruption showing the evolution of time-average discharge rate (TADR), volume, area, area change (dArea), and mean thickness. Orange boxes denote uncertainty in measurement. Blue crosses denote supporting TADR measurements (Text S3 in Supporting Information S1).

Phase 1 of the eruption (19 March–5 April) began when a 180 m long fissure opened on 19 March between 20:30 (tremor started) and 20:50 (first visual confirmation) in the Geldingadalir valley, which is located east of Mt. Fagradalsfjall (Figure 1). Soon the eruption concentrated on two neighboring vents and the lava started infilling the valley (Figure 2a). During this phase, the TADR ranged from 1 to 8 m³/s with a mean for the entire phase of  $4.9 \pm 0.1$  m³/s (Figure 2b). The lava area increased to 0.33 km², while the mean thickness increased to 22 m reaching a lava volume of  $7.0 \pm 0.2 \times 10^6$  m³ before Phase 2 started.

PEDERSEN ET AL. 4 of 11



In Phase 2 (5–27 April) the active vent migrated. Multiple fissures opened, starting on 5 April (Figure 1, vent 2), when two new fissures opened 800 m northeast of the first fissure. Another fissure opened at midnight on 7 April (vent 3), another one on 10 April (vent 4) and then again on 13 April when two new fissures opened (vents 5 and 6). Each fissure concentrated into 1–2 circular vents, which over the following 10 days became inactive, except for the southern vents that developed from the April 13 fissure. Phase 2 had similar TADR as in Phase 1, in the range 5–8 m³/s, with the highest TADR observed just after new vent openings. The mean TADR in this period was  $6.3 \pm 0.4$  m³/s and the cumulative volume increased to  $19.4 \pm 0.8 \times 10^6$  m³. With the migration of active vent locations, lava started to flow into the valleys of Meradalir (5 April) and Syðri-Meradalur (14 April) covering an area of 1.1 km² with a mean thickness of 16 m.

In Phase 3 (27 April–28 June) the vent activity stabilized at one location. Most of the time (2 May–12 June) it exhibited cycles of short-term pulsations observed on webcams and tremor graphs. The TADR increased from 9 to a maximum of 13 m³/s with a phase mean of  $11.4 \pm 0.5$  m³/s. The "fill and spill" from one valley into another increased the area stepwise to 3.82 km² with mean thickness of 20.8 m yielding a total volume of  $79.8 \pm 1.5 \times 10^6$  m³. The lava migrated to Nátthagi valley through Syðri-Meradalir (22 May) and through southern Geldingadalir (13 June).

Phase 4 (28 June–2 September) was characterized by episodic activity with intense lava emplacement (ca. 12–24 hr) followed by inactive periods of similar length documented by webcams and tremor graphs. Despite the episodic activity this period had only slightly lower TADR than Phase 3 with a mean for the whole phase of  $11.0 \pm 0.4$  m³/s ranging from 8.5 to 11.1 m³/s and the cumulative volume increased to  $142.5 \pm 1.4 \times 10^6$  m³. The lava thickened to around 50 m northeast of the active crater due to episodic overflows and in Meradalir the lava thickened by ~25 m due to stacking and inflation.

The eruption's rhythm changed again in the final phase, Phase 5 (2–18 September), when a 9-day long pause from 2 to 11 September, was followed by week-long period of activity from 11 to 18 September. The measured TADR was 12 m³/s for 9–17 September. The mean TADR for Phase 5 is  $5.6 \pm 0.6$  m³/s and the total volume increased to  $150.8 \pm 2.7 \times 10^6$  m³. Most of the deposition was in Geldingadalir, where a 10–15 m thick lava pond was established north-northwest of the active crater between 11 and 15 September, that partly drained through an upwelling zone toward south and into Nátthagi from 15 to 18 September.

## 3.2. Monitoring of Lava Flow-Field and Transport Systems

The extent of the lava field and the lava transport system was controlled by the complex topography of the Fagradalsfjall area, and lava pathways were confined to the valleys and the steep slopes connecting them (Figure S5 in Supporting Information S1). The expansion of the lava flow field was closely tied to the fill and spill of lava from one valley to another and thus short-term prediction of the timing of valley overflow became important.

Overall, this monitoring was two-fold; (a) Mapping of the lava extent and the filling of the valleys, and (b) Rate of volume change into different valleys.

The monitoring of the lava extent and the filling of the valleys could be directly evaluated based on the products from the photogrammetric surveys. The lava expansion was mapped by plotting the lava outlines and the filling of valleys could be monitored by plotting topographic profiles along potential lava pathway exits based on the DEMs derived from each survey (Figure 3a). The infilling of Geldingardalir and Nátthagi were particularly important because overflow could endanger sections of hiking paths, critical communication cables and an important highway.

Lava discharge into different valleys was highly variable switching from one valley to another as revealed by the infilling of the valleys (Figure 3a). It was important to estimate this variability to make short-term prediction of valley overflows and for lava flow modeling. The rate of volume change,  $\Delta V/\Delta t$ , into each valley could be calculated by integrating the thickness change retrieved from the lava thickness change map within five flow field zones (Figure 3b).

In phase 3–4 the rate of volume change into individual valleys could increase two - threefold between surveys (Figure 3b) although the total TADR in phase 3–4 (Figure 2) was similar. The change in Phase 5 was 5 to 10-fold for Geldingardalir. These changes provided great challenges for forecasting the timing of lava spilling from one valley to another.

PEDERSEN ET AL. 5 of 11



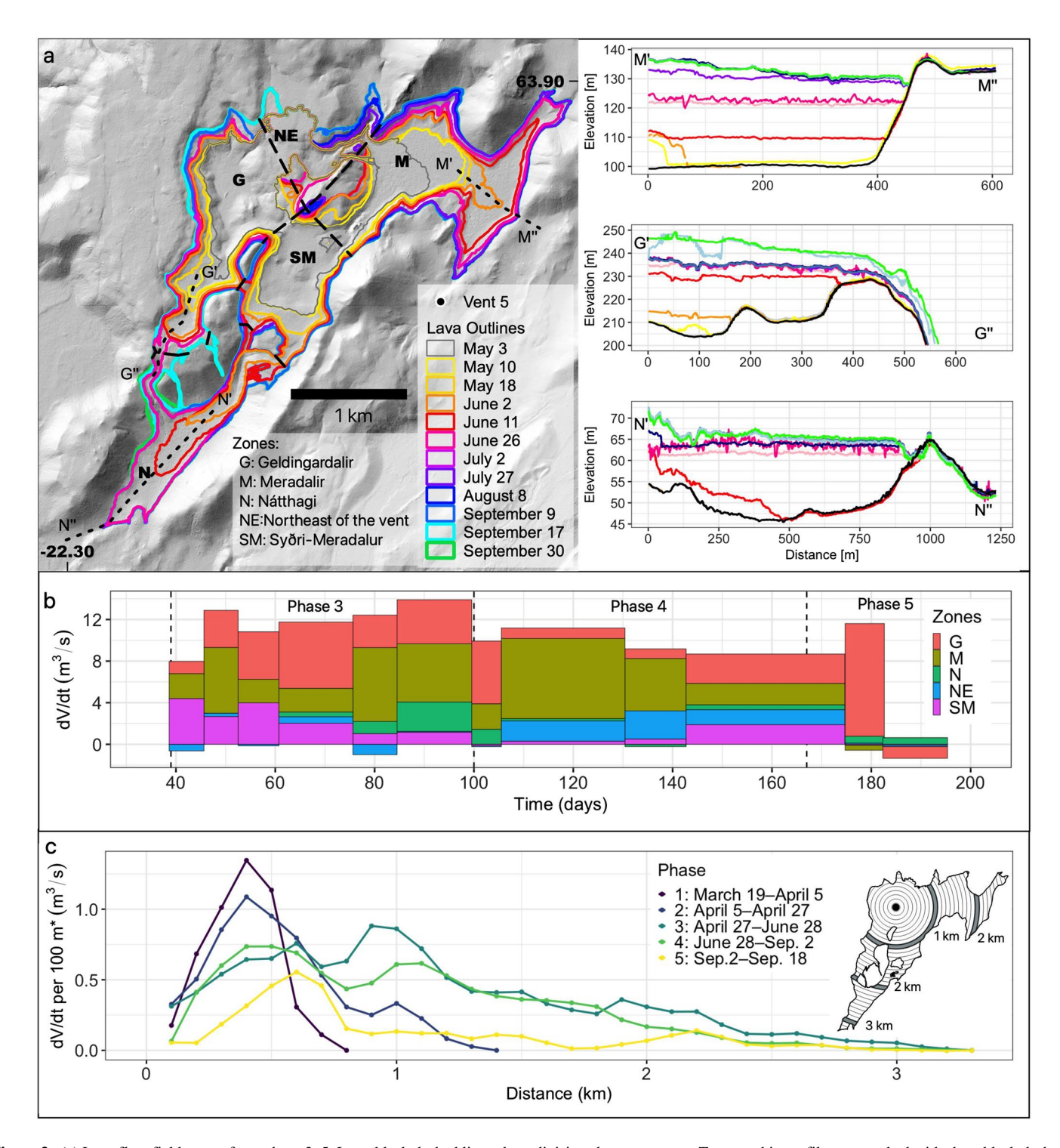


Figure 3. (a) Lava flow field extent from phase 3–5. Long black dashed lines show divisions between zones. Topographic profiles are marked with short black dashed line and shown for Meradalir, Geldingardalir and Nátthagi and use the same color scheme for lava flow field extent. The black topographic profile is pre-eruption topography. (b) The rate of volume change,  $\Delta V/\Delta t$ , into different zones. (c) The lava flow field expansion for each phase illustrated by the rate of volume change,  $\Delta V/\Delta t$ , for every 100 m interval, as a function of distance from the vent 5. The star (\*, y-axis title) denotes that it is per 100 m radially from the vent.

Similarly, the rate of volume change at a specific vent distance (at 100 m interval) can be calculated. This allows us to investigate the expansion of the lava flow field based on the TADR changes observed for each eruption phase (Figure 3c). In Phase 1, all lava was emplaced within Geldingadalir, reaching a distance of 800 m from the vent, while reaching 1,400 m from the vents in Phase 2 as new vents opened. The mean TADR increased from

PEDERSEN ET AL. 6 of 11



5 to 6 m³/s in phases 1–2 to 11 m³/s in Phase 3, causing the lava flow field to expand to its maximum extent at 3.3 km from the vent (Figure 3c). Similar mean TADR and maximum deposition distance was observed in Phase 4. However, compared to Phase 3 less lava was deposited in the far field, suggesting that the change from continuous (Phase 3) to episodic activity (Phase 4) at the vent impacted the lava transport system and the ability of the lava field to expand. In Phase 5, most lava emplacement was within a 1 km radius of the active vent but reached 3.1 km in mid-September after the drainage of a pond northwest of the crater (Figure 3c).

#### 4. Discussion

Satellite and airborne photogrammetry provided flexible methods for near real-time monitoring of volume and TADR on a daily to weekly basis for Icelandic conditions. The 3D maps and TADR estimates were used extensively by Civil Protection when informing local authorities, police, and other responders during regular briefings. The TADR results and the evolving lava topography also provided constraints for lava flow simulations and estimates of when lava might flow out of the valleys of Meradalir and Nátthagi.

### 4.1. Effusion Rate Evolution and Plumbing System

Different trends in effusion rate evolution have been classified into types and linked to specific plumbing system dynamics (Aravena et al., 2020; Harris et al., 2000, 2011). Type I is characterized by a phase of high initial effusion followed by an extended phase of waning effusion (initial eruption rate/mean output rate >1 and t50/t100 < 0.5, where  $t_k$  represents the time required to evacuate the k percent of the total erupted mass), which has been interpreted as a tapping of a pressurized reservoir (Wadge, 1981) and efficient magma ascent in early stages (Aravena et al., 2020). Type II has a low, near-constant effusion rate (initial eruption rate/mean output rate  $\approx 1$  and  $t50/t100 \approx 0.5$ ) and has been related to low initial overpressure (5–10 MPa), consistent with overflow in a non-pressurized system (Aravena et al., 2020; Harris et al., 2000). In type III eruptions, the effusion rate increases with time (initial eruption rate/mean output rate 1 and t50/t1000.5) and has been suggested to be linked with ascent of a magma batch, pushing a volume of degassed magma ahead (Harris et al., 2011). However, this trend has also been linked to conduit erosion caused by high erosion coefficients, high initial overpressures, and/or large magma reservoirs (Aravena et al., 2020). The last type is type IV, which shows highly pulsating effusion rate and has been related to ascent of multiple batches of magma (Harris et al., 2011).

The Fagradalsfjall 2021 eruption started with a low and stable effusion rate between 4 and 8 m<sup>3</sup>/s in phase 1–2 (Figure 2) and initially had the characteristics of a type II eruption. However, in phase 3–4 the effusion rate increased to 8–13 m<sup>3</sup>/s changing the characteristics to resemble a type III eruption. The low initial effusion rate at Fagradalsfjall is between 30 and 2500 times smaller than other recorded Icelandic eruptions in the last 75 years (Gudmundsson et al., 2004, 2012; Hreinsdóttir et al., 2014; Jude-Eton et al., 2012; Pedersen et al., 2017, 2018; Thorarinsson, 1967; Thorarinsson et al., 1964). However, it is not only a low initial eruption rate that is unusual, but the evolution of the effusion rate at Fagradalsfjall, which is unlike any observations from previous recent Icelandic eruptions (Figures 4a and 4b).

Fagradalsfjall 2021 eruption is the first time we observed a type III eruption, compared to other recent Icelandic eruptions that show characteristics of type I eruptions. Based on the interpretation of type I eruptions (Wadge, 1981), it makes sense that eruptions in Hekla, Grímsvötn and Bárðarbunga (Holuhraun 2014–2015) all show eruption rate evolution controlled by pressurized reservoirs, since these are very active volcanic systems that show evidence of having magma chambers (e.g., Geirsson et al., 2012; Gudmundsson et al., 2016; Hreinsdóttir et al., 2014; Ofeigsson et al., 2011). Less information exists for the Vestmannaeyjar volcanic system responsible for the Surtsey 1963–1967 eruption, but based on the available data (Thorarinsson et al., 1964), the effusion rate evolution suggests that Fagradalsfjall is unlike this eruption as well. Whether this difference is linked to the tectonic setting of an oblique spreading rift, the thin crustal thickness of western Reykjanes Peninsula (Allen et al., 2002), or if it may be special for the Fagradalsfjall volcanic system, which is unlike the other volcanic systems on the Reykjanes Peninsula, requires further investigation.

The evolution of the effusion rate of type III eruptions has been linked to the ascent of a single magma batch, pushing a volume of degassed magma ahead (Harris et al., 2011; Steffke et al., 2011). Interestingly, geochemical evidence suggests that in phase 1–2 the magma plumbing system gradually changed from being fed from a

PEDERSEN ET AL. 7 of 11



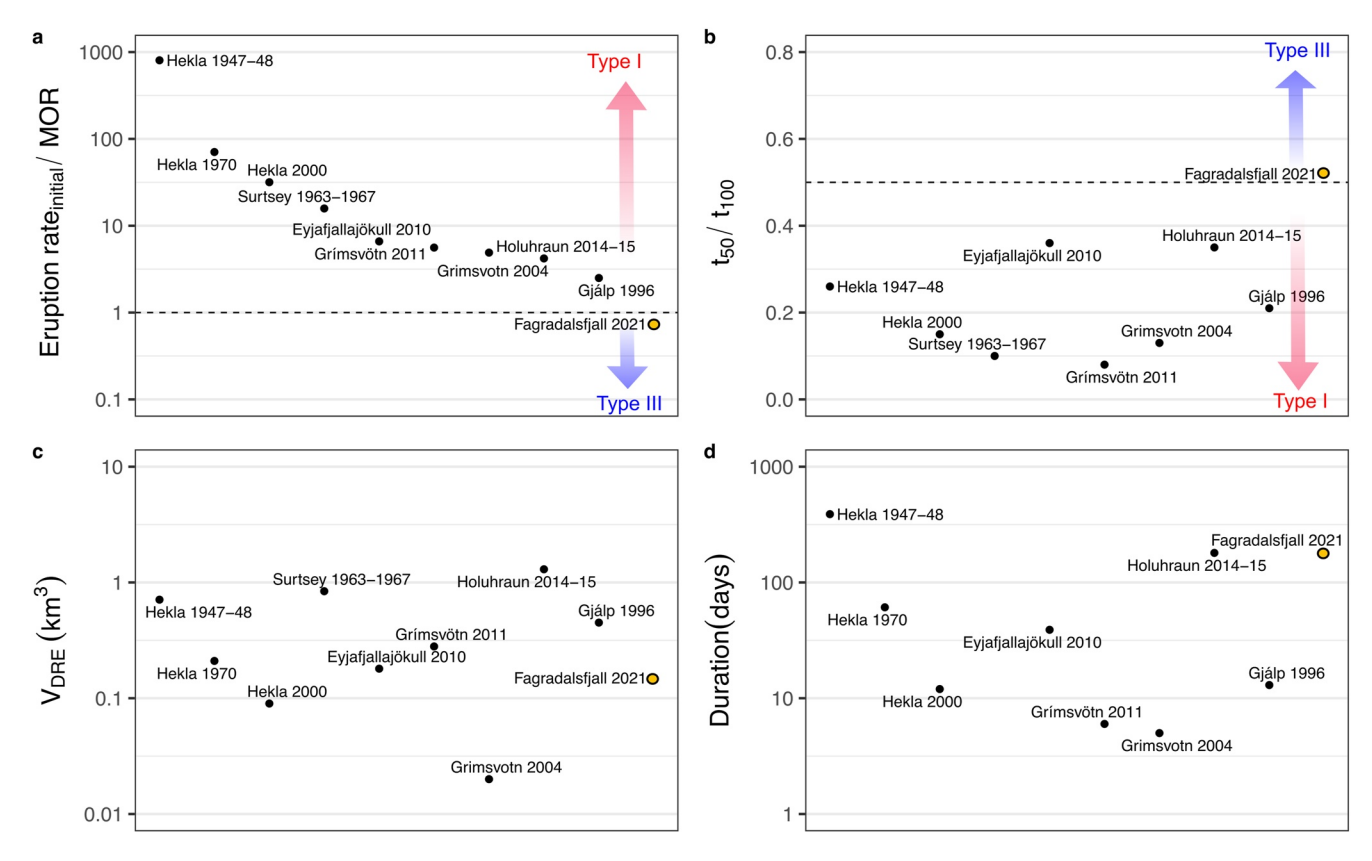


**Figure 4.** Fagradalsfjall eruption parameter characteristics compared to other recent Icelandic eruptions (Gudmundsson et al., 2004, 2012; Hreinsdóttir et al., 2014; Jude-Eton et al., 2012; Pedersen et al., 2017, 2018; Thorarinsson, 1967; Thorarinsson et al., 1964). (a) Normalizing the initial eruption rate (used here because instead of effusion rate since the eruptions both include effusive and explosive eruptions) with the mean output rate (Harris et al., 2007). Fagradalsfjall 2021 is clearly an outlier with a ratio below 1. The effusion rate evolution of types I and III (Harris et al., 2000, 2011) have been indicated in red and blue arrows. Type II should ideally plot along the dashed line, while the pulsating nature of type IV could plot everywhere in the plot. (b)  $t_{50}/t_{100}$ . Types I and III have been indicated in red and blue arrows, type II should ideally plot along 0.5. Fagradalsfjall plot between type II and III. (c) Total erupted volume (Dry Rock Equivalent, DRE). (d) Eruption duration.

depleted shallow mantle source to being fed by more enriched discrete melts lenses from greater depth by day 40 (Marshall et al., 2021), while the increase in TADR was observed between day 40 and 50.

The delay between the geochemical change and the increased effusion is intriguing. In the 2018 Kīlauea eruption the increase in effusion started within a day of an observed change to more mafic magma increasing the effusion from 7 m³/s to 110 m³/s (Dietterich et al., 2021; Gansecki et al., 2019). Furthermore, this change was associated with observed deformation and earthquake activity. Thus, there was a clear link between a change in geochemistry and a substantial increase in effusion.

However, if the effusion increase in Fagradalsfjall is related to ascent of a magma batch pushing a degassed magma ahead (which would be  $\sim 20 \times 10^6$  m³ based on the erupted bulk volume estimates at day 40), then it clearly was a more subtle process compared to the 2018 Kīlauea eruption, potentially involving lower overpressure and slower increase in effusion.

The increase in effusion can also be explained by thermal erosion of the conduit, which is consistent with fairly high  $t_{50}/t_{100}$  values (Figure 4b, Aravena et al., 2020). The eruption in phase 1–2 displayed type II characteristics, consistent with overflow in a non-pressurized magma reservoir. Over time, the heating of the conduit walls enabled sufficient thermal erosion to increase the effusion rate, which for a cylindrical conduit is proportional to  $r^4$ , where r is radius (e.g., Aravena et al., 2020; Turcotte & Schubert, 2002). This process may have been enhanced by the increased temperature of the magma due to an increase in MgO from 8.8% to 9.7% (Marshall et al., 2021).

We consider this conduit-controlled flow a plausible model for Fagradalsfjall, because such a model, along with the geochemical evidence of deep-rooted feeding of distributed melt-lenses (Marshall et al., 2021), explains the

PEDERSEN ET AL. 8 of 11



sharp contrast with the behavior to other Icelandic eruptions (e.g., Hekla, Grímsvötn and Bárðarbunga) where pressure in a magma chamber is considered the main control of flow (e.g., Hreinsdóttir et al., 2014).

#### 5. Conclusions

Near real-time photogrammetric monitoring of the eruption at Fagradalsfjall 2021 was performed using a combination of satellite and airborne stereoimages. This provided essential eruption parameters such as volume and effusion rate, as well as the maps which were distributed to the public, the Civil Protection, rescue teams, and the tourism industry.

By 30 September 2021, 32 surveys had been performed. The lava flow field covered 4.8 km<sup>2</sup> and the estimated bulk volume (including vesicles and macroscale porosity) is  $150 \times 10^6$  m<sup>3</sup>, yielding a mean output rate of  $9.5 \pm 0.2$  m<sup>3</sup>/s (from 19 March to 18 September 2021).

The lava pathways and lava advancement were complex and changeable, as the lava filled and spilled from one valley into another and short-term prediction of the timing of overflow from one valley to another proved challenging.

Compared to recent Icelandic eruptions, the evolution of the effusion rate is very unusual, having a very low and stable effusion in phase 1–2 and increasing effusion in Phase 3. This behavior may be due to change in magma widening of the conduit by thermal erosion with time, and not controlled by magma chamber pressure as is most common in the volcanic zones of Iceland.

# **Data Availability Statement**

The DEMs, orthoimages and lava outlines are available in https://zenodo.org/record/6598466 (Pedersen et al., 2022).

# Acknowledgments References

The authors would like to thank reviewer

Hannah Dietterich and editor Chris-

tian Huber for constructive comments

improving this manuscript. Extended

thanks goes to the pilots Ú. Hennings-

son, K. Kárason, K. Halldórsdóttir, G.

Coast Guard and Iceland Aviation Service for their commitment to carry out flights.

The authors acknowledge the Icelandic Research fund, Grant Nos. 206755-052,

program, NSF RAPID program and the

French Space Agency (CNES) for their

support. Pléiades images were provided

during the first 10 days of the eruption

Committee on Earth Observing Satellites

(image Pléiades@CNES2021, distribution

under the CIEST2 (CNES) initiative

and through the Icelandic Volcanoes

Supersite project supported by the

AIRBUS DS).

the Fulbright-NSF Arctic Scholar

Árnason, J. Sverrisson, the Icelandic

Allen, R. M., Nolet, G., Morgan, W. J., Vogfjörd, K., Nettles, M., Ekström, G., et al. (2002). Plume-driven plumbing and crustal formation in Iceland. *Journal of Geophysical Research*, 107, ESE 4-1–ESE 4-19. https://doi.org/10.1029/2001jb000584

Aravena, A., Cioni, R., Coppola, D., Vitturi, M. M., Neri, A., Pistolesi, M., & Ripepe, M. (2020). Effusion rate evolution during small-volume basaltic eruptions: Insights from numerical modeling. *Journal of Geophysical Research: Solid Earth*, 125(6), e2019JB019301. https://doi.org/10.1029/2019JB019301

Belart, J. M. C., Magnússon, E., Berthier, E., Pálsson, F., Aðalgeirsdóttir, G., & Jóhannesson, T. (2019). The geodetic mass balance of Eyjafjallajökull ice cap for 1945–2014: Processing guidelines and relation to climate. *Journal of Glaciology*, 65, 395–409. https://doi.org/10.1017/jog/2019/16

Calvari, S. (2019). Understanding lava flow morphologies and structures for hazard assessment. *Annals of Geophysics*, 61. https://doi.org/10.4401/

Clifton, A. E., & Kattenhorn, S. A. (2006). Structural architecture of a highly oblique divergent plate boundary segment. *Tectonophysics*, 419(1), 27–40. https://doi.org/10.1016/j.tecto.2006.03.016

Dietterich, H. R., Diefenbach, A. K., Soule, S. A., Zoeller, M. H., Patrick, M. P., Major, J. J., & Lundgren, P. R. (2021). Lava effusion rate evolution and erupted volume during the 2018 Kīlauea lower East Rift Zone eruption. *Bulletin of Volcanology*, 83(4), 25. https://doi.org/10.1007/s00445-021-01443-6

Einarsson, P., Eyjólfsson, V., & Hjartardóttir, Á. R. (2022). Fault structures in the Fagradalsfjall area and tectonic framework of the 2021 eruption in the Reykjanes Peninsula oblique rift, Iceland. *Nordic Geological Winter Meeting, Reykjavík, Iceland*.

Einarsson, P., Hjartardóttir, Á. R., Imsland, P., & Hreinsdóttir, S. (2020). The structure of seismogenic strike-slip faults in the eastern part of the Reykjanes Peninsula Oblique Rift, SW Iceland. *Journal of Volcanology and Geothermal Research*, 391. 106372. https://doi.org/10.1016/j.jvolgeores.2018.04.029

Gansecki, C., Lee, R. L., Shea, T., Lundblad, S. P., Hon, K., & Parcheta, C. (2019). The tangled tale of Kīlauea's 2018 eruption as told by geochemical monitoring. *Science*, 366(6470). eaaz0147. https://doi.org/10.1126/science.aaz0147

Gee, M. A. M. (1998). Volcanology and geochemistry of Reykjanes Peninsula: Plume-mid-ocean ridge interaction [PhD]. University of London. Geirsson, H., LaFemina, P., Árnadóttir, T., Sturkell, E., Sigmundsson, F., Travis, M., et al. (2012). Volcano deformation at active plate boundaries: Deep magma accumulation at Hekla volcano and plate boundary deformation in south Iceland. Journal of Geophysical Research, 117(B11). B11409. https://doi.org/10.1029/2012JB009400

Gudmundsson, M. T., Jónsdóttir, K., Hooper, A., Holohan, E. P., Halldórsson, S. A., Ófeigsson, B. G., et al. (2016). Gradual caldera collapse at Bárdarbunga volcano, Iceland regulated by lateral magma outflow. *Science*, 353, aaf8988. https://doi.org/10.1126/science.aaf8988

Gudmundsson, M. T., Sigmundsson, F., Björnsson, H., & Högnadóttir, T. (2004). The 1996 eruption at Gjálp, Vatnajökull ice cap, Iceland: Efficiency of heat transfer, ice deformation and subglacial water pressure. *Bulletin of Volcanology*, 66(1), 46–65. https://doi.org/10.1007/s00445-003-0295-9

Gudmundsson, M. T., Thordarson, T., Höskuldsson, Á., Larsen, G., Björnsson, H., Prata, A. J., et al. (2012). Ash generation and distribution from the April–May 2010 eruption of Eyjafjallajökull, Iceland. Scientific Reports, 2, 572. https://doi.org/10.1038/srep00572

PEDERSEN ET AL. 9 of 11



- Harris, A., Steffke, A., Calvari, S., & Spampinato, L. (2011). Thirty years of satellite-derived lava discharge rates at Etna: Implications for steady volumetric output. *Journal of Geophysical Research*, 116(B8). B08204. https://doi.org/10.1029/2011JB008237
- Harris, A. J. L., Dehn, J., & Calvari, S. (2007). Lava effusion rate definition and measurement: A review. *Bulletin of Volcanology*, 70(1), 1. https://doi.org/10.1007/s00445-007-0120-y
- Harris, A. J. L., Murray, J. B., Aries, S. E., Davies, M. A., Flynn, L. P., Wooster, M. J., et al. (2000). Effusion rate trends at Etna and Krafla and their implications for eruptive mechanisms. *Journal of Volcanology and Geothermal Research*, 102(3), 237–269. https://doi.org/10.1016/S0377-0273(00)00190-6
- Höhle, J., & Höhle, M. (2009). Accuracy assessment of digital elevation models by means of robust statistical methods. ISPRS Journal of Photogrammetry and Remote Sensing, 64, 398–406. https://doi.org/10.1016/j.isprsjprs.2009.02.003
- Hreinsdóttir, S., Sigmundsson, F., Roberts, M. J., Björnsson, H., Grapenthin, R., Arason, T., et al. (2014). Volcanic plume height correlated with magma-pressure change at Grímsvötn Volcano, Iceland. *Nature Geoscience*, 7, 214–218. https://doi.org/10.1038/ngeo2044
- Jones, J. G. (1969). Intraglacial volcanoes of the Laugarvatn region, south-west Iceland—I. Quarterly Journal of the Geological Society, 124(1-4), 197-211. https://doi.org/10.1144/gsjgs.124.1.0197
- Jude-Eton, T. C., Thordarson, T., Gudmundsson, M. T., & Oddsson, B. (2012). Dynamics, stratigraphy and proximal dispersal of supraglacial tephra during the ice-confined 2004 eruption at Grímsvötn volcano, Iceland. *Bulletin of Volcanology*, 74, 1057–1082. https://doi.org/10.1007/ s00445-012-0583-3
- Klein, F. W., Einarsson, P., & Wyss, M. (1977). The Reykjanes Peninsula, Iceland, earthquake swarm of September 1972 and its tectonic significance. *Journal of Geophysical Research*, 82(5), 865–888. https://doi.org/10.1029/JB082i005p00865
- Marshall, E. W., Rasmussen, M. B., Halldorsson, S. A., Matthews, S., Ranta, E., Sigmarsson, O., et al. (2021). Rapid geochemical evolution of the mantle-sourced Fagradalsfjall eruption, Iceland. AGU Fall Meeting, New Orleans, USA.
- Ofeigsson, B. G., Hooper, A., Sigmundsson, F., Sturkell, E., & Grapenthin, R. (2011). Deep magma storage at Hekla volcano, Iceland, revealed by InSAR time series analysis. *Journal of Geophysical Research*, 116(B5). B05401. https://doi.org/10.1029/2010JB007576
- Pedersen, G. B. M., Belart, J. M. C., Magnússon, E., Vilmundardóttir, O. K., Kizel, F., Sigurmundsson, F. S., et al. (2018). Hekla volcano, Iceland, in the 20th century: Lava volumes, production rates, and effusion rates. Geophysical Research Letters, 45(4), 1805–1813. https://doi.org/10.1002/2017GL076887
- Pedersen, G. B. M., Belart, J. M. C., Óskarsson, B. V., Gudmundsson, M. T., Gies, N., Högnadóttir, T., et al. (2022). Digital Elevation Models, orthoimages and lava outlines of the 2021 Fagradalsfjall eruption: Results from near real-time photogrammetric monitoring (Version v1.1) [Dataset]. Zenodo. https://doi.org/10.5281/zenodo.6598466
- Pedersen, G. B. M., & Grosse, P. (2014). Morphometry of subaerial shield volcanoes and glaciovolcanoes from Reykjanes Peninsula, Iceland: Effects of eruption environment. *Journal of Volcanology and Geothermal Research*, 282, 115–133. https://doi.org/10.1016/j.jvolgeores. 2014.06.008
- Pedersen, G. B. M., Höskuldsson, A., Dürig, T., Thordarson, T., Jónsdóttir, I., Riishuus, M. S., et al. (2017). Lava field evolution and emplacement dynamics of the 2014–2015 basaltic fissure eruption at Holuhraun, Iceland. *Journal of Volcanology and Geothermal Research*, 340, 155–169. https://doi.org/10.1016/j.jvolgeores.2017.02.027
- Pierrot Deseilligny, M., & Clery, I. (2011). Apero, an open source bundle adjustment software for automatic calibration and orientation of set of images. The International Archives of the Photogrammetry, Remote Sensing and Spatial Information Sciences, 3816, 269–276. https://doi. org/10.5194/isprsarchives-XXXVIII-5-W16-269-2011
- Poland, M. P. (2014). Time-averaged discharge rate of subaerial lava at Kīlauea Volcano, Hawai'i, measured from TanDEM-X interferometry: Implications for magma supply and storage during 2011–2013. *Journal of Geophysical Research: Solid Earth*, 119(7), 5464–5481. https://doi.org/10.1002/2014JB011132
- Porter, C., Morin, P., Howat, I., Noh, M.-J., Bates, B., Peterman, K., et al. (2018). *ArcticDEM. Harvard dataverse, V1*. Polar Geospatial Center, University of Minnesota. https://doi.org/10.7910/DVN/OHHUKH
- Rupnik, E., Daakir, M., & Pierrot Deseilligny, M. (2017). MicMac A free, open-source solution for photogrammetry. *Open Geospatial Data*, Software Standards, 2, 14. https://doi.org/10.1186/s40965-017-0027-2
- Sæmundsson, K., & Sigurgeirsson, M. Á. (2013). Reykjanesskagi. In J. Sólnes, F. Sigmundsson, & B. Bessason (Eds.), Náttúruvá (pp. 379–401). Viðlagatrygging Íslands / Háskólaútgáfa.
- Sæmundsson, K., Sigurgeirsson, M. Á., & Friðleifsson, G. Ó. (2020). Geology and structure of the Reykjanes volcanic system, Iceland. *Journal of Volcanology and Geothermal Research*, 391, 106501. https://doi.org/10.1016/j.jvolgeores.2018.11.022
- Shean, D. E., Alexandrov, O., Moratto, Z. M., Smith, B. E., Joughin, I. R., Porter, C., & Morin, P. (2016). An automated, open-source pipeline for mass production of digital elevation models (DEMs) from very-high resolution commercial stereo satellite imagery. ISPRS Journal of Photogrammetry and Remote Sensing, 116, 101–117. https://doi.org/10.1016/j.isprsjprs.2016.03.012
- Steffke, A. M., Harris, A. J. L., Burton, M., Caltabiano, T., & Salerno, G. G. (2011). Coupled use of COSPEC and satellite measurements to define the volumetric balance during effusive eruptions at Mt. Etna, Italy. *Journal of Volcanology and Geothermal Research*, 205(1), 47–53. https://doi.org/10.1016/j.jvolgeores.2010.06.004
- Thórarinsson, S. (1967). The eruption of Hekla 1947–1948 I: The eruptions of Hekla in historical times. A tephrocronological study (pp. 1–171). Societas Scientarium Islandica.
- Thorarinsson, S., Einarsson, T., Sigvaldason, G., & Elisson, G. (1964). The submarine eruption off the Vestmann islands 1963–64 A preliminary report. *Bulletin Volcanologique*, 27, 435–445. https://doi.org/10.1007/BF02597544
- Turcotte, D. L., & Schubert, G. (2002). Geodynamics (2nd ed., p. 56). University Press.
- Wadge, G. (1981). The variation of magma discharge during basaltic eruptions. *Journal of Volcanology and Geothermal Research*, 11(2), 139–168. https://doi.org/10.1016/0377-0273(81)90020-2
- Walker, G. P. L. (1973). Lengths of lava flows. Philosophical Transactions of the Royal Society A: Mathematical, Physical & Engineering Sciences, 274, 107–118. https://doi.org/10.1098/rsta.1973.0030

# **References From the Supporting Information**

- Gardelle, J., Berthier, E., Arnaud, Y., & Kääb, A. (2013). Region-wide glacier mass balances over the Pamir-Karakoram-Himalaya during 1999–2011. The Cryosphere, 7, 1263–1286. https://doi.org/10.5194/tc-7-1263-2013
- Gudmundsson, M. T., Högnadóttir, Þ., Kristinsson, A. B., & Gudbjörnsson, S. (2007). Geothermal activity in the subglacial Katla caldera, Iceland, 1999–2005, studied with radar altimetry. Annals of Glaciology, 45, 66–72. https://doi.org/10.3189/172756407782282444

PEDERSEN ET AL. 10 of 11



10.1029/2021GL097125



- Jóhannesson, T., Björnsson, H., Magnusson, E., Gudmundsson, S., Palsson, F., Sigurdsson, O., et al. (2013). Ice-volume changes, bias estimation of mass-balance measurements and changes in subglacial lakes derived by lidar mapping of the surface of Icelandic glaciers. *Annals of Glaciology*, 54(63), 63–74.
- Nuth, C., & Kääb, A. (2011). Co-registration and bias corrections of satellite elevation data sets for quantifying glacier thickness change. *The Cryosphere*, 5, 271–290. https://doi.org/10.5194/tc-5-271-2011
- Óskarsson, B. V., Jónasson, K., Valsson, G., & Belart, J. M. C. (2020). Erosion and sedimentation in Surtsey Island quantified from new DEMs. Surtsey Research, 14, 63–77. https://doi.org/10.33112/surtsey.14.5
- Shean, D., & Bhushan, S. (2021). Chamoli disaster pre-event DEM (2015-05-07 WorldView-1 stereo) (Version 1) [Dataset]. Zenodo. https://doi.org/10.5281/zenodo.4533679
- Sørensen, E. V., & Dueholm, M. (2018). Analytical procedures for 3D mapping at the photogeological laboratory of the geological survey of Denmark and Greenland. *Geological Survey of Denmark and Greenland Bulletin*, 41, 99–104. https://doi.org/10.34194/geusb.v41.4353

PEDERSEN ET AL. 11 of 11